Measurement of the Michel parameters and the ν_τ helicity in τ lepton decays

The ALEPH Collaboration[*]

Abstract

A measurement of the Michel parameters and the average ν_τ helicity in τ lepton decays is described. The data was collected with the ALEPH detector at LEP during the years 1991 to 1995. A total integrated luminosity of $155\,\mathrm{pb}^{-1}$ is analysed. The Michel parameters ρ_l, ξ_l, $(\xi\delta)_l$ $(l = e, \mu)$, and η_μ are determined for the leptonic decays, and the chirality parameters ξ_π, ξ_ρ, and ξ_{a_1} for the hadronic final states. Under the assumptions of e-μ universality and $\xi_\pi = \xi_\rho = \xi_{a_1}$, the values $\rho_l = 0.742 \pm 0.016, \eta_l = 0.012 \pm 0.026, (\xi\delta)_l = 0.776 \pm 0.051, \xi_l = 0.986 \pm 0.074$, and $\xi_h = 0.992 \pm 0.011$ are obtained. No significant deviation is observed from the Standard Model assumption of the $\mathrm{V} - \mathrm{A}$ structure of the charged weak interaction.

To be submitted to The European Physical Journal C

---

[*]See next pages for the list of authors.

The ALEPH Collaboration

A. Heister, S. Schael

  Physikalisches Institut das RWTH-Aachen, D-52056 Aachen, Germany

R. Barate, I. De Bonis, D. Decamp, C. Goy, J.-P. Lees, E. Merle, M.-N. Minard, B. Pietrzyk

  Laboratoire de Physique des Particules (LAPP), IN^2P^3-CNRS, F-74019 Annecy-le-Vieux Cedex, France

S. Bravo, M.P. Casado, M. Chmeissani, J.M. Crespo, E. Fernandez, M. Fernandez-Bosman, Ll. Garrido,[15] E. Graugés, M. Martinez, G. Merino, R. Miquel,[27] Ll.M. Mir,[27] A. Pacheco, H. Ruiz

  Institut de Física d'Altes Energies, Universitat Autònoma de Barcelona, E-08193 Bellaterra (Barcelona), Spain[7]

A. Colaleo, D. Creanza, M. de Palma, G. Iaselli, G. Maggi, M. Maggi, S. Nuzzo, A. Ranieri, G. Raso,[23] F. Ruggieri, G. Selvaggi, L. Silvestris, P. Tempesta, A. Tricomi,[3] G. Zito

  Dipartimento di Fisica, INFN Sezione di Bari, I-70126 Bari, Italy

X. Huang, J. Lin, Q. Ouyang, T. Wang, Y. Xie, R. Xu, S. Xue, J. Zhang, L. Zhang, W. Zhao

  Institute of High Energy Physics, Academia Sinica, Beijing, The People's Republic of China[8]

D. Abbaneo, P. Azzurri, G. Boix,[6] O. Buchmüller, M. Cattaneo, F. Cerutti, B. Clerbaux, G. Dissertori, H. Drevermann, R.W. Forty, M. Frank, T.C. Greening, J.B. Hansen, J. Harvey, P. Janot, B. Jost, M. Kado, P. Mato, A. Moutoussi, F. Ranjard, L. Rolandi, D. Schlatter, O. Schneider,[2] P. Spagnolo, W. Tejessy, F. Teubert, E. Tournefier,[25] J. Ward

  European Laboratory for Particle Physics (CERN), CH-1211 Geneva 23, Switzerland

Z. Ajaltouni, F. Badaud, A. Falvard,[22] P. Gay, P. Henrard, J. Jousset, B. Michel, S. Monteil, J-C. Montret, D. Pallin, P. Perret, F. Podlyski

  Laboratoire de Physique Corpusculaire, Université Blaise Pascal, IN^2P^3-CNRS, Clermont-Ferrand, F-63177 Aubière, France

J.D. Hansen, J.R. Hansen, P.H. Hansen, B.S. Nilsson, A. Wäänänen

  Niels Bohr Institute, DK-2100 Copenhagen, Denmark[9]

A. Kyriakis, C. Markou, E. Simopoulou, A. Vayaki, K. Zachariadou

  Nuclear Research Center Demokritos (NRCD), GR-15310 Attiki, Greece

A. Blondel,[12] G. Bonneaud, J.-C. Brient, A. Rougé, M. Rumpf, M. Swynghedauw, M. Verderi, H. Videau

  Laboratoire de Physique Nucléaire et des Hautes Energies, Ecole Polytechnique, IN^2P^3-CNRS, F-91128 Palaiseau Cedex, France

V. Ciulli, E. Focardi, G. Parrini

  Dipartimento di Fisica, Università di Firenze, INFN Sezione di Firenze, I-50125 Firenze, Italy

A. Antonelli, M. Antonelli, G. Bencivenni, G. Bologna,[4] F. Bossi, P. Campana, G. Capon, V. Chiarella, P. Laurelli, G. Mannocchi,[5] F. Murtas, G.P. Murtas, L. Passalacqua, M. Pepe-Altarelli[24]

  Laboratori Nazionali dell'INFN (LNF-INFN), I-00044 Frascati, Italy

A.W. Halley, J.G. Lynch, P. Negus, V. O'Shea, C. Raine, A.S. Thompson

  Department of Physics and Astronomy, University of Glasgow, Glasgow G12 8QQ,United Kingdom[10]

S. Wasserbaech

  Department of Physics, Haverford College, Haverford, PA 19041-1392, U.S.A.

R. Cavanaugh, S. Dhamotharan, C. Geweniger, P. Hanke, G. Hansper, V. Hepp, E.E. Kluge, A. Putzer, J. Sommer, K. Tittel, S. Werner,[19] M. Wunsch[19]

Kirchhoff-Institut für Physik, Universität Heidelberg, D-69120 Heidelberg, Germany[16]

R. Beuselinck, D.M. Binnie, W. Cameron, P.J. Dornan, M. Girone,[1] N. Marinelli, J.K. Sedgbeer, J.C. Thompson[14]

Department of Physics, Imperial College, London SW7 2BZ, United Kingdom[10]

V.M. Ghete, P. Girtler, E. Kneringer, D. Kuhn, G. Rudolph

Institut für Experimentalphysik, Universität Innsbruck, A-6020 Innsbruck, Austria[18]

E. Bouhova-Thacker, C.K. Bowdery, A.J. Finch, F. Foster, G. Hughes, R.W.L. Jones,[1] M.R. Pearson, N.A. Robertson

Department of Physics, University of Lancaster, Lancaster LA1 4YB, United Kingdom[10]

I. Giehl, K. Jakobs, K. Kleinknecht, G. Quast, B. Renk, E. Rohne, H.-G. Sander, H. Wachsmuth, C. Zeitnitz

Institut für Physik, Universität Mainz, D-55099 Mainz, Germany[16]

A. Bonissent, J. Carr, P. Coyle, O. Leroy, P. Payre, D. Rousseau, M. Talby

Centre de Physique des Particules, Université de la Méditerranée, IN²P³-CNRS, F-13288 Marseille, France

M. Aleppo, F. Ragusa

Dipartimento di Fisica, Università di Milano e INFN Sezione di Milano, I-20133 Milano, Italy

A. David, H. Dietl, G. Ganis,[26] K. Hüttmann, G. Lütjens, C. Mannert, W. Männer, H.-G. Moser, R. Settles, H. Stenzel, W. Wiedenmann, G. Wolf

Max-Planck-Institut für Physik, Werner-Heisenberg-Institut, D-80805 München, Germany[16]

J. Boucrot,[1] O. Callot, M. Davier, L. Duflot, J.-F. Grivaz, Ph. Heusse, A. Jacholkowska,[22] J. Lefrançois, J.-J. Veillet, I. Videau, C. Yuan

Laboratoire de l'Accélérateur Linéaire, Université de Paris-Sud, IN²P³-CNRS, F-91898 Orsay Cedex, France

G. Bagliesi, T. Boccali, G. Calderini, L. Foà, A. Giassi, F. Ligabue, A. Messineo, F. Palla, G. Sanguinetti, A. Sciabà, G. Sguazzoni, R. Tenchini,[1] A. Venturi, P.G. Verdini

Dipartimento di Fisica dell'Università, INFN Sezione di Pisa, e Scuola Normale Superiore, I-56010 Pisa, Italy

G.A. Blair, G. Cowan, M.G. Green, T. Medcalf, A. Misiejuk, J.A. Strong, P. Teixeira-Dias, J.H. von Wimmersperg-Toeller

Department of Physics, Royal Holloway & Bedford New College, University of London, Egham, Surrey TW20 OEX, United Kingdom[10]

R.W. Clifft, T.R. Edgecock, P.R. Norton, I.R. Tomalin

Particle Physics Dept., Rutherford Appleton Laboratory, Chilton, Didcot, Oxon OX11 OQX, United Kingdom[10]

B. Bloch-Devaux,[1] P. Colas, S. Emery, W. Kozanecki, E. Lançon, M.-C. Lemaire, E. Locci, P. Perez, J. Rander, J.-F. Renardy, A. Roussarie, J.-P. Schuller, J. Schwindling, A. Trabelsi,[21] B. Vallage

CEA, DAPNIA/Service de Physique des Particules, CE-Saclay, F-91191 Gif-sur-Yvette Cedex, France[17]

N. Konstantinidis, A.M. Litke, G. Taylor

Institute for Particle Physics, University of California at Santa Cruz, Santa Cruz, CA 95064, USA[13]

C.N. Booth, S. Cartwright, F. Combley, M. Lehto, L.F. Thompson

Department of Physics, University of Sheffield, Sheffield S3 7RH, United Kingdom[10]

K. Affholderbach, A. Böhrer, S. Brandt, C. Grupen, A. Ngac, G. Prange, U. Sieler

Fachbereich Physik, Universität Siegen, D-57068 Siegen, Germany[16]

G. Giannini

Dipartimento di Fisica, Università di Trieste e INFN Sezione di Trieste, I-34127 Trieste, Italy

J. Rothberg

Experimental Elementary Particle Physics, University of Washington, Seattle, WA 98195 U.S.A.

S.R. Armstrong, K. Cranmer, P. Elmer, D.P.S. Ferguson, Y. Gao,[20] S. González, O.J. Hayes, H. Hu, S. Jin, J. Kile, P.A. McNamara III, J. Nielsen, W. Orejudos, Y.B. Pan, Y. Saadi, I.J. Scott, J. Walsh, Sau Lan Wu, X. Wu, G. Zobernig

Department of Physics, University of Wisconsin, Madison, WI 53706, USA[11]

1 Introduction

The decay of the τ lepton, mediated through the weak charged current, is described in the Standard Model by a pure V − A interaction. For the μ decay, the V − A assumption has already been confirmed with high precision [1, 2] by the determination of its Michel parameters and complementary measurements. The aim of this analysis of the τ decays is to look for small deviations from the electroweak prediction of the Standard Model which could arise from new physics. The measured parameters are the Michel parameters for leptonic decays and chirality parameters ξ_h, related to the ν_τ helicity, for hadronic decays.

The τ leptons are produced in the process $e^+e^- \rightarrow \tau^+\tau^-$ and have correlated helicities. Their decays into the final states $e^-\bar{\nu}_e\nu_\tau$, $\mu^-\bar{\nu}_\mu\nu_\tau$, $\pi^-(K^-)\nu_\tau$, $\pi^-\pi^0\nu_\tau$, $\pi^-\pi^0\pi^0\nu_\tau$, $\pi^-\pi^+\pi^-\nu_\tau$, and the charge conjugate states are analysed. This measurement uses the full data sample collected with the ALEPH detector from the LEP runs around the Z resonance corresponding to an integrated luminosity of $155\,\mathrm{pb}^{-1}$. It supersedes earlier results from ALEPH [3] based on a smaller data sample. To achieve the best sensitivity, the τ rest frame is reconstructed when possible, namely in the case of both τ's decaying hadronically.

2 Lorentz structure and definition of the parameters

2.1 Leptonic decays

The matrix element of the most general four-fermion contact interaction used to describe the purely leptonic decay $\tau^- \rightarrow l^-\bar{\nu}_l\nu_\tau$ [4–7] can be written in the helicity projection formalism as [8, 9]

$$\mathcal{M} = 4\frac{G_l}{\sqrt{2}} \sum_{\substack{\gamma=S,V,T \\ i,j=R,L}} g_{ij}^\gamma \langle \bar{l}_i|\Gamma^\gamma|(\nu_l)_n\rangle\langle(\bar{\nu}_\tau)_m|\Gamma_\gamma|\tau_j\rangle, \qquad (l=e,\mu). \qquad (1)$$

The constant G_l is the absolute coupling strength and the g_{ij}^γ are ten ($g_{ii}^T = 0$) complex coupling constants describing the relative contribution of scalar ($\Gamma^S = 1$), vector ($\Gamma^V = \gamma^\mu$), and tensor ($\Gamma^T = \frac{1}{\sqrt{2}}\sigma^{\mu\nu}$) interactions respectively, for given chiralities j, i of the τ and the charged decay lepton. The neutrino chiralities n and m are then uniquely defined for a given set γ, i, j. The V − A interaction assumed in the Standard Model corresponds in this formalism to $g_{LL}^V = 1$ and $g_{ij}^\gamma = 0$ for all other couplings. The matrix element (1) can be used to compute the spectrum of the charged decay lepton. When the final state polarisation is integrated out, the spectrum is described by four real parameters[1] ρ, η, ξ, and $\xi\delta$, the Michel parameters.

To express the relation between the Michel parameters and the g_{ij}^γ coupling constants, it is helpful to introduce the six positive parameters

---

[1] The original parameters [5] were $\alpha = \xi/3 - 4\xi\delta/9$ and $\beta = \xi\delta/3$. Employing ξ and δ [7] gives a more symmetrical shape to the formulae but δ is not bounded. Using ξ and $\xi\delta$ as independent parameters retains the advantages of the two formulations

$$\begin{aligned}
\alpha^+ &= |g_{RL}^V|^2 + |g_{RL}^S + 6g_{RL}^T|^2/16 \ , \\
\alpha^- &= |g_{LR}^V|^2 + |g_{LR}^S + 6g_{LR}^T|^2/16 \ , \\
\beta^+ &= |g_{RR}^V|^2 + |g_{RR}^S|^2/4 \ , \\
\beta^- &= |g_{LL}^V|^2 + |g_{LL}^S|^2/4 \ , \\
\gamma^+ &= (3/16)|g_{RL}^S - 2g_{RL}^T|^2 \ , \\
\gamma^- &= (3/16)|g_{LR}^S - 2g_{LR}^T|^2 \ ,
\end{aligned}$$

(2)

(3)

(4)

where $\pm$ denotes the final state charged lepton chirality. The normalization condition reads

$$\alpha^+ + \alpha^- + \beta^+ + \beta^- + \gamma^+ + \gamma^- = \sum_{i,j} \left(|g_{ij}^V|^2 + \frac{1}{4}|g_{ij}^S|^2 + 3\,|g_{ij}^T|^2 \right) = 1 \ . \qquad (5)$$

The ρ, ξ, and $\xi\delta$ parameters are given by

$$\begin{aligned}
\rho &= \frac{3}{4}(\beta^+ + \beta^-) + (\gamma^+ + \gamma^-) \ , \\
\xi &= 3\,(\alpha^- - \alpha^+) + (\beta^- - \beta^+) + \frac{7}{3}(\gamma^+ - \gamma^-) \ , \\
\xi\delta &= \frac{3}{4}(\beta^- - \beta^+) + (\gamma^+ - \gamma^-) \ .
\end{aligned}$$

(6)

The Standard Model prediction ($|g_{LL}^V| = 1$ and all the other $g_{ij}^\gamma = 0$) implies $\beta^- = 1$, hence $\xi = 1$, $\rho = \xi\delta = 3/4$ but the converse is not true, and ambiguities affect the τ left-handed couplings. The upper limits of these couplings, compatible with the Standard Model values of ρ, ξ, and $\xi\delta$ [10], are given in Table 1.

Table 1: Values of the coupling constants for left-handed τ's in the Standard Model compared to their absolute maximum values and to the upper limits compatible with the Standard Model prediction: $\xi = 1$, $\rho = \xi\delta = 3/4$

	$|g_{RL}^S|$	$|g_{LL}^S|$	$|g_{RL}^V|$	$|g_{LL}^V|$	$|g_{RL}^T|$
SM	0	0	0	1	0
absolute maximum	2	2	1	1	$1/\sqrt{3}$
maximum when $\rho = \xi\delta = 3/4$, $\xi = 1$	2	2	1/2	1	1/2

Since the physically interesting region is the neighbourhood of the Standard Model prediction, no relevant information on the non-standard τ left-handed couplings can be extracted from the measurement of ρ, ξ, and $\xi\delta$. The right-handed couplings, on the contrary, are constrained by two independent linear combinations of the parameters whose vanishing implies that all the g_{iR}^γ are equal to zero, for instance:

$$\mathcal{S}_R^\tau = \frac{2}{3}[\rho - \xi\delta] = \beta^+ + \frac{4}{3}\gamma^- = \frac{1}{4}\,(|g_{RR}^S|^2 + |g_{LR}^S - 2g_{LR}^T|^2) + |g_{RR}^V|^2 \ , \qquad (7)$$

2

$$\mathcal{P}_R^\tau = \frac{1}{2}[1 + \frac{\xi}{3} - \frac{16}{9}\xi\delta] = \beta^+ + \alpha^- + \gamma^- \tag{8}$$

$$= \frac{1}{4}(|g_{RR}^S|^2 + |g_{LR}^S|^2) + |g_{RR}^V|^2 + |g_{LR}^V|^2 + 3|g_{LR}^T|^2 ,$$

where the last combination $\mathcal{P}_R^\tau$ is the fractional contribution of the τ right-handed couplings to the leptonic partial width. Therefore the Michel parameters are sensitive to the existence of heavy W bosons with right-handed couplings predicted by left-right symmetric models [11].

The last Michel parameter η, which vanishes in the Standard Model, receives a contribution from the interference between the dominant g_{LL}^V coupling and a scalar coupling which could be due to a charged Higgs boson [12, 13]. It can be written

$$\eta \simeq \frac{1}{2}\mathrm{Re}(g_{RR}^S g_{LL}^{V*}) , \tag{9}$$

keeping only the the dominant term. It is the sole Michel parameter which contributes to the τ leptonic partial widths [9]:

$$\Gamma_l \simeq \frac{m_\tau^5 G_l^2}{192\pi^3}[1 + 4\eta_l \frac{m_l}{m_\tau}] . \tag{10}$$

The energy spectrum of the charged lepton in the laboratory system is:

$$(1 + 4\eta_l \frac{m_l}{m_\tau})\frac{1}{\Gamma}\frac{d\Gamma}{dx} = f(x; \rho_l, \eta_l) + P_\tau\, g(x; \xi_l, (\xi\delta)_l) \tag{11}$$

$$= f_0(x) + \eta_l\, f_\eta(x) + \rho_l\, f_\rho(x) + P_\tau\,[\xi_l g_\xi(x) + (\xi\delta)_l\, g_{\xi\delta}(x)] ,$$

where P_τ is the τ polarisation and $x = E_l/E_\mathrm{beam}$ the normalized lepton energy. The functions f and g describe the "isotropic", and the τ helicity dependent parts of the spectrum, respectively. Neglecting radiative corrections and higher order terms in m_l/m_τ allows f and g to be expressed as polynomials in x,

$$f(x) = \frac{1}{3}\Big[(5 - 9x^2 + 4x^3) - \frac{4}{3}[\rho_l - \frac{3}{4}](1 - 9x^2 + 8x^3) + 36\frac{m_l}{m_\tau}\eta_l(1 - x)^2\Big], \tag{12}$$

$$g(x) = \frac{1}{3}\Big[\xi_l(1 - 9x^2 + 8x^3) - \frac{4}{3}[(\xi\delta)_l - \frac{3}{4}\xi_l](1 - 12x + 27x^2 - 16x^3)\Big] . \tag{13}$$

Since the term involving η_l in Eq. 12 contains a factor m_l/m_τ, the contribution of η_l is largely suppressed, especially for the electron, where the suppression factor is about 3×10^{-4}. Therefore there is no sensitivity to η_e with the statistics available today.

2.2 Hadronic decays

●   For the simplest decay mode $\tau^- \to \pi^-\nu_\tau$, there is only one observable, the τ decay angle, related to the pion energy in the laboratory by $\cos\theta \simeq 2x_\pi - 1$, with $x_\pi = E_\pi/E_\mathrm{beam}$. The decay distribution reads

$$\frac{1}{\Gamma}\frac{d\Gamma}{d\cos\theta}(\tau^- \to \pi^-\nu_\tau) = \frac{1}{2}[1 + \xi_\pi P_\tau \cos\theta] , \tag{14}$$

3

where the chirality parameter ξ_π is related to the average ν_τ helicity by $\langle h_{\nu_\tau} \rangle = -\xi_\pi$.

- For the decay $\tau^- \to \pi^- \pi^0 \nu_\tau$ (ρ decay), the set of observables is $\vec{x} = (Q^2, \cos\theta, \alpha, \beta)$, where Q^2 is the squared invariant mass of the hadronic $(\pi^- \pi^0)$ system, θ the τ decay angle, α and β the azimuthal and polar angles of the π^- with respect to the τ direction in the hadronic centre-of-mass system. The decay distribution reads

$$\frac{1}{\Gamma}\frac{d\Gamma}{d\vec{x}}(\tau^- \to \pi^- \pi^0 \nu_\tau) = F_\rho(\vec{x}) + \xi_\rho P_\tau \, G_\rho(\vec{x}) \ . \tag{15}$$

Using the reduced optimal variable [14] $\omega_\rho = G_\rho/F_\rho$, the distribution becomes

$$\frac{1}{\Gamma}\frac{d\Gamma}{d\omega_\rho}(\tau^- \to \pi^- \pi^0 \nu_\tau) = f_\rho(\omega_\rho)(1 + \xi_\rho P_\tau \omega_\rho) = f_\rho(\omega_\rho) + \xi_\rho P_\tau g_\rho(\omega_\rho) \ . \tag{16}$$

If the τ rest frame is not reconstructed, α is not measured and β is relative to the ρ line of flight in the laboratory. If only V and A couplings are present, the functions F_ρ and G_ρ are determined by Lorentz invariance only without further hypothesis. The construction of the ω_ρ variable used in the present study utilizes these functions.

The effect of possible other couplings is more simply understood when the τ rest frame is reconstructed. In this case, transverse ($\lambda_\rho = \pm 1$) and longitudinal ($\lambda_\rho = 0$) ρ's can be statistically separated through the $\cos\beta$ distribution which is proportional to $\sin^2\beta$ for transverse and to $\cos^2\beta$ for longitudinal $\rho's$. As in the case of the π decay mode, the decay distributions are

$$\frac{1}{\Gamma^{L/T}}\frac{d\Gamma^{L/T}}{d\cos\theta}(\tau^- \to \rho^- \nu_\tau) = \frac{1}{2}[1 \pm \xi_\rho^{L/T} P_\tau \cos\theta] \ , \tag{17}$$

with the same relation as for $\tau \to \pi\nu_\tau$ between the ξ parameters and the average neutrino helicity. The nature of the coupling affects only the proportions of transverse and longitudinal ρ's. Since scalar couplings cannot contribute to ρ production, the two possibilities are vector and tensor couplings. They give, irrespectively of the ν_τ helicity, amplitudes in the ratio $A^T/A^L = \sqrt{2}m/m_\tau$ for vector and $A^T/A^L = \sqrt{2}m_\tau/m$ for tensor [15], if the neutrino mass is negligible compared to the $\pi^- \pi^0$ effective mass m. The $\cos\beta$ distribution when the τ rest frame is reconstructed depends only on $|A^T/A^L|^2$ and is the most sensitive observable to the presence of tensor couplings. The agreement (Fig. 1) between the $\cos\beta$ distribution observed in the data and that predicted by the Standard Model Monte Carlo supports the use of the chosen parametrization.

- For the decay $\tau^- \to 3\pi\nu_\tau$ (a_1 decay), the parameters used to describe the final state are [16] $\vec{x} = (Q^2, \cos\theta, s_1, s_2, \alpha, \beta, \gamma)$, where s_1 and s_2 are the squared invariant masses of the unlike-sign two-pion systems and α, β, and γ three Euler angles which specify the direction of the normal to the three-pion system decay plane and the orientation of one of the pions in this plane. Here also, the measurement of α requires the reconstruction of the τ rest frame. Since, in the case of three pions, it is possible to construct pseudo-scalar quantities from the pion momenta only, the decay distribution assumes a more complex form:

$$\frac{1}{\Gamma}\frac{d\Gamma}{d\vec{x}}(\tau^- \to 3\pi\nu_\tau) = F_{a_1}(\vec{x}) + \xi_{a_1} P_\tau \, G^1_{a_1}(\vec{x}) + \xi_{a_1} G^2_{a_1}(\vec{x}) + P_\tau \, G^3_{a_1}(\vec{x}) \ . \tag{18}$$
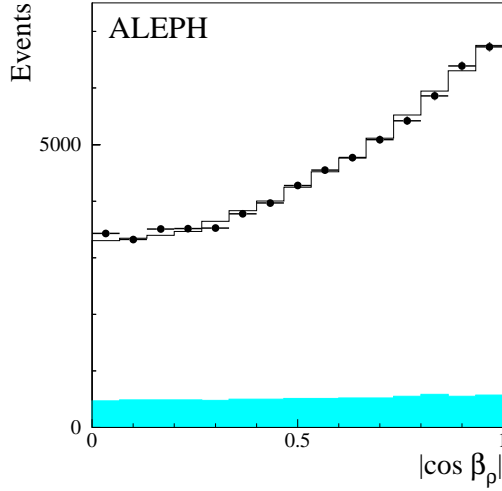
4

Figure 1: Distribution of the ρ decay angle when the τ rest frame is reconstructed. The points are data, the full line is the expectation from Monte Carlo, and the shaded area the contribution of τ background

If the decay is described by the reduced variable $\omega_{a_1} = G^1_{a_1}/F_{a_1}$ [14], the functions $G^2_{a_1}$ and $G^3_{a_1}$, which contain the above mentioned pseudo-scalar quantities, are integrated out and the decay distribution reads

$$\frac{1}{\Gamma}\frac{d\Gamma}{d\omega_{a_1}}(\tau^- \to 3\pi\nu_\tau) = f_{a_1}(\omega_{a_1})(1 + \xi_{a_1}P_\tau\omega_{a_1}) = f_{a_1}(\omega_{a_1}) + \xi_{a_1}P_\tau g_{a_1}(\omega_{a_1}) \ . \qquad (19)$$

Even with only V and A couplings, the complexity of the final state introduces some hadronic model dependence in the definition of the F_{a_1} and $G^i_{a_1}$ functions used to compute ω_{a_1} [16]. Accordingly, the determination of ξ_{a_1} presented here is affected by theoretical systematic uncertainties. Other measurements of ξ_{a_1} [17–19] use only the pseudo-scalar observable of the 3π final state [20]. They are also affected by theoretical systematic effects, but these effects are not correlated to the theoretical uncertainties on the present measurement since they rest on the knowledge of the $G^2_{a_1}$ function which is not used here.

● As previously mentioned, the computation of the ω variables used in this analysis assumes that only V and A couplings intervene. The matrix element is written

$$\mathcal{M} = \cos\theta_c \frac{G}{\sqrt{2}} \langle \bar{\nu}_\tau | \gamma_\mu (g_V - g_A\gamma_5)|\tau\rangle \langle J^\mu\rangle \qquad (20)$$

for a Cabibbo favoured decay. The nature of the hadronic current J^μ is determined by the hadronic final state. The chirality parameters ξ_h ($h = \pi, \rho, a_1$) are then given by

$$\xi_h = 2\mathrm{Re}(g_V g_A^*)/(|g_V|^2 + |g_A|^2) \ . \qquad (21)$$

In the Standard Model $\xi_h = 1$.

5

2.3   Correlated decays

With the reduced ω variables, the decay distribution has the same expression for all the hadronic decays:

$$\frac{1}{\Gamma}\frac{d\Gamma}{d\omega_h}(\tau^- \to h^-\nu_\tau) = f_h(\omega_h) + \xi_h P_\tau g_h(\omega_h) \qquad (h = \pi, \rho, a_1) \;, \tag{22}$$

where $\omega_\pi = \cos\theta \simeq 2x_\pi - 1$. From Equations 11 to 13 and 22, it is clear that the measurement of the decay parameters from single τ decay spectra requires the knowledge of the polarisation. Alternatively, the full correlation between the spins of the τ^+ and the τ^- in an event can be exploited [21, 22] to measure the parameters by the fit of the $\tau^+\tau^-$ two-dimensional correlated decay spectra. Since $P_\tau = P_{\tau^-} = -P_{\tau^+}$ and since CP invariance implies that all the ξ_l and ξ_h parameters have opposite values for τ^+ and τ^-, while ρ, η, and δ are the same, the correlated spectra can be written in terms of the τ^- polarisation and decay parameters as

$$\frac{1}{\Gamma}\frac{d^2\Gamma}{d\omega_{h_1}d\omega_{h_2}} = f_{h_1}(\omega_{h_1})f_{h_2}(\omega_{h_2}) + \xi_{h_1}\xi_{h_2}\,g_{h_1}(\omega_{h_1})g_{h_2}(\omega_{h_2}) \tag{23}$$

$$+P_\tau\{\xi_{h_1}\,g_{h_1}(\omega_{h_1})f_{h_2}(\omega_{h_2}) + \xi_{h_2}\,f_{h_1}(\omega_{h_1})g_{h_2}(\omega_{h_2})\}\;,$$

$$(1 + 4\eta_l\frac{m_l}{m_\tau})\frac{1}{\Gamma}\frac{d^2\Gamma}{dx_l d\omega_h} = [f_0(x_l) + \eta_l f_\eta(x_l)]f_h(\omega_h) + \xi_l\xi_h\,[g_\xi(x_l) + \delta_l g_{\xi\delta}(x_l)]g_h(\omega_h) \tag{24}$$

$$+P_\tau\{\xi_l\,[g_\xi(x_l) + \delta_l g_{\xi\delta}(x_l)]f_h(\omega_h) + \xi_h\,[f_0(x_l) + \eta_l f_\eta(x_l)]g_h(\omega_h)\}\;,$$

for hadron-hadron and lepton-hadron correlations respectively.

All the parameters can be measured in this way with only a global sign ambiguity on the ξ parameters and P_τ. This ambiguity is resolved by comparing, for instance, the determinations of the Z couplings to electrons from the τ polarisation forward-backward asymmetry [23] and from the beam polarisation left-right asymmetry [24].

The complete correlation of the τ^+ and τ^- helicities is a consequence of the Standard Model. Nevertheless, if only CP invariance is assumed and the helicity correlation coefficient is written $-\chi$, the distributions (23) and (24) keep the same form with effective parameters $\xi_{h/l}^{\mathrm{eff}} = \sqrt{\chi}\xi_{h/l}$ and $P_\tau^{\mathrm{eff}} = P_\tau/\sqrt{\chi}$. Since[2] $|\xi_h| \le 1$, the observation of effective hadronic parameters equal to one implies both $\xi_h = 1$ and $\chi = 1$.

3   Apparatus

The ALEPH detector is described in detail in [25] and its performance in [26].

Charged particles are measured with a high resolution silicon vertex detector (VDET), a cylindrical drift chamber (ITC), and a large time projection chamber (TPC). The momentum resolution in the axial magnetic field of 1.5 T provided by a superconducting solenoid is $\Delta p/p^2 = 0.6 \times 10^{-3}(\mathrm{GeV}/c)^{-1}$ for high momentum tracks. The impact

---

[2]Even if, in the case of the a_1, ξ_h is regarded as a mere phenomenological parameter, the positivity of the probability distribution (19) implies $|\xi_h| \le 1$

parameter resolutions for tracks with hits in all three subdetectors are $\sigma_{r\phi} = 23\,\mu\mathrm{m}$ and $\sigma_z = 28\,\mu\mathrm{m}$.

The tracking devices are surrounded by the electromagnetic calorimeter (ECAL), which is a highly segmented lead/proportional-wire-chamber calorimeter. The calorimeter is read out via cathode pads arranged in projective towers covering $0.9° \times 0.9°$ in solid angle and summing the deposited energy in three sections of depth. A second read-out is provided by the signals from the anode wires. The energy resolution is $\sigma/E = 0.009 + 0.18/\sqrt{E}\,(\mathrm{GeV})$.

Outside the ECAL lies the solenoid, which is followed by the hadron calorimeter (HCAL). Hadronic showers are sampled by 23 planes of streamer tubes giving a digital hit pattern and an analog signal on pads, which are also arranged in projective towers. This calorimeter is used to discriminate between pions and muons. Outside the HCAL there are two layers of muon chambers providing additional information for μ identification.

4 Event selection

The selection of $\tau\tau$ events is based on the algorithm described in [27] and [28]. It starts by dividing the event in two hemispheres by a plane perpendicular to the thrust axis. Cuts are then applied on the characteristics of the "jets" reconstructed in each hemisphere and the particle identification is used to improve the rejection of e-e and μ-μ pairs. The overall efficiency of this selection is $(77.99 \pm 0.23)\%$ with a remaining non-τ background of $(0.8 \pm 0.1)\%$, composed mainly of Bhahba events (0.28%), μ pairs (0.08%), hadrons (0.25%), and events from $\gamma\gamma$ interactions (0.17%). These are average numbers, the actual background depends on the τ final states and is properly taken into account (see Table 2).

The next step in the selection procedure is the identification of the various τ decays (Table 3). It relies mainly on the particle identification algorithm and the fake photon estimator developed for the τ polarisation measurement, which are described in detail in [23] and summarized below. A good photon is defined either as an electromagnetic cluster found by the photon clustering algorithm [29] and not rejected by the fake photon estimator, or as a conversion consisting of two tracks with a reconstructed vertex, very low invariant mass, and at least one identified electron. For the reconstruction of a π^0, an invariant mass between $0.08\,\mathrm{GeV}/c^2$ and $0.22\,\mathrm{GeV}/c^2$ is required. To improve the energy resolution, the accepted π^0 candidates are kinematically fitted to their nominal mass, if the two photons are electromagnetic clusters [29].

$\boldsymbol{\tau^- \to l^- \nu_\tau \bar{\nu}_l}$

A hemisphere is called e or μ if it has exactly one good track [23] identified as an electron or a muon. In addition no $\gamma\gamma$ pair with an invariant mass compatible with a π^0 should be found.

$\boldsymbol{\tau^- \to \pi^- \nu_\tau}$

For this final state, the hemisphere must have exactly one good track with a momentum greater than $2\,\mathrm{GeV}/c$, identified as a pion [23], and there should be no good photon. Cuts on the ratios of the calorimetric energies to the momentum of the track measured in the TPC are also applied to reduce the remaining background from electrons.

7

Table 2: Efficiencies, background from τ decays and from non-τ events for the final states (inclusive and correlated) used in the analysis. All numbers are given in percent, the errors are only statistical

| Class | Efficiency | Background | |
		τ decays	non-τ
e	70.88 ± 0.11	1.12 ± 0.03	1.03 ± 0.07
e-e	62.66 ± 0.40	2.23 ± 0.15	3.04 ± 0.42
e-μ	67.25 ± 0.28	3.11 ± 0.12	0.02 ± 0.02
e-π	55.26 ± 0.36	9.11 ± 0.27	0.14 ± 0.08
e-ρ	57.88 ± 0.24	12.47 ± 0.20	0.19 ± 0.06
e-$\pi 2\pi^0$	39.81 ± 0.40	24.35 ± 0.48	0.07 ± 0.07
e-$3\pi^\pm$	55.35 ± 0.41	9.70 ± 0.32	0.00 ± 0.00
μ	75.88 ± 0.11	1.80 ± 0.04	0.54 ± 0.05
μ-μ	71.08 ± 0.39	3.90 ± 0.19	2.92 ± 0.42
μ-π	58.78 ± 0.36	9.40 ± 0.27	0.14 ± 0.08
μ-ρ	61.97 ± 0.24	13.43 ± 0.20	0.04 ± 0.03
μ-$\pi 2\pi^0$	42.89 ± 0.41	24.30 ± 0.47	0.00 ± 0.00
μ-$3\pi^\pm$	58.43 ± 0.41	10.61 ± 0.32	0.00 ± 0.00
π	60.41 ± 0.15	7.82 ± 0.10	0.08 ± 0.03
π-π	42.47 ± 0.62	16.69 ± 0.66	0.00 ± 0.00
π-ρ	49.12 ± 0.30	18.25 ± 0.30	0.05 ± 0.04
π-$\pi 2\pi^0$	33.28 ± 0.47	30.18 ± 0.67	0.00 ± 0.00
π-$3\pi^\pm$	46.40 ± 0.51	16.40 ± 0.51	0.00 ± 0.00
ρ	63.26 ± 0.10	11.72 ± 0.08	0.07 ± 0.02
ρ-ρ	50.94 ± 0.29	22.26 ± 0.30	0.03 ± 0.02
ρ-$\pi 2\pi^0$	34.84 ± 0.33	32.69 ± 0.45	0.05 ± 0.05
ρ-$3\pi^\pm$	46.66 ± 0.34	19.80 ± 0.36	0.03 ± 0.03
$\pi 2\pi^0$	42.66 ± 0.17	23.74 ± 0.20	0.03 ± 0.02
$\pi 2\pi^0$-$\pi 2\pi^0$	23.50 ± 0.68	42.53 ± 0.24	0.00 ± 0.00
$\pi 2\pi^0$-$3\pi^\pm$	30.94 ± 0.53	31.58 ± 0.79	0.01 ± 0.01
$3\pi^\pm$	57.79 ± 0.17	8.99 ± 0.13	0.02 ± 0.01
$3\pi^\pm$-$3\pi^\pm$	39.55 ± 0.81	17.79 ± 0.91	0.00 ± 0.00

$\tau^- \to \rho^- \nu_\tau \to \pi^- \pi^0 \nu_\tau$

Two cases are distinguished. Firstly, if there is one π^0 and no additional good photon, one good track is required and a cut $0.3 \, \text{GeV}/c^2 < m_{\pi\pi^0} < 1.6 \, \text{GeV}/c^2$ is applied. Secondly, since for a high energy π^0 it is probable that the two photons are merged into one cluster, it might happen that only one good photon is found. Then the hemisphere should have one good track identified as a pion and fulfil the same mass cut as above.

$\tau^- \to a_1^- \nu_\tau \to \pi^- \pi^0 \pi^0 \nu_\tau$

As for the two-pion final state several cases are considered. Besides the requirement of one good track in the hemisphere there should be either two π^0's, or one π^0 and one

good photon, or two good photons. In the last case the track must be identified as a pion. In addition the following mass cuts are applied: $0.6\,\mathrm{GeV}/c^2 < m_{\pi\pi^0} < 1.2\,\mathrm{GeV}/c^2$ and $m_{\pi\pi^0\pi^0} < m_\tau$.

$$\tau^- \to a_1^- \nu_\tau \to \pi^- \pi^+ \pi^- \nu_\tau$$

The hemisphere must have three good tracks with at least one track identified as pion, no good photon, one $\pi^+\pi^-$ invariant mass greater than $0.56\,\mathrm{GeV}/c^2$, and an invariant mass of the 3π system smaller than the τ mass.

Besides events with both hemispheres classified, events with only one identified hemisphere are also retained if the unknown hemisphere (X) has exactly one or three good charged tracks. The results of the selection and the number of events used in the analysis can be found in Tables 2 and 3.

Table 3: The 27 decay combinations and the number of reconstructed events (Unidentified hemispheres are labelled X)

Class	Events	Class	Events	Class	Events
e-e	4106	μ-ρ	12311	ρ-ρ	8059
e-μ	8379	μ-$\pi 2\pi^0$	3228	ρ-$\pi 2\pi^0$	4305
e-π	4897	μ-$3\pi^\pm$	3715	ρ-$3\pi^\pm$	4868
e-ρ	11686	μ-X	8435	ρ-X	11386
e-$\pi 2\pi^0$	3051	π-π	1293	$\pi 2\pi^0$-$\pi 2\pi^0$	588
e-$3\pi^\pm$	3627	π-ρ	6689	$\pi 2\pi^0$-$3\pi^\pm$	1298
e-X	8431	π-$\pi 2\pi^0$	1785	$\pi 2\pi^0$-X	2972
μ-μ	4543	π-$3\pi^\pm$	2046	$3\pi^\pm$-$3\pi^\pm$	680
μ-π	5056	π-X	4771	$3\pi^\pm$-X	3305
		Total number of events used:		135510	

5   Reconstruction of the τ direction of flight

As already mentioned in Section 1, the full sensitivity of the decay distributions with two and three pions in the final state can only be exploited if the τ lepton rest frame is known. This requires the reconstruction of the τ direction of flight in the laboratory.

In events with both τ leptons decaying hadronically, under the assumption that no photon is radiated in the τ production process, the reconstruction of the directions of the τ momenta $\vec{\mathbf{k}}_+$ and $\vec{\mathbf{k}}_-$ from the four-momenta $(E_+, \vec{\mathbf{p}}_+)$ and $(E_-, \vec{\mathbf{p}}_-)$ of the two hadronic systems (Fig. 2) is possible by means of the following equations [30]:

$$\hat{\mathbf{k}}_+ = -\hat{\mathbf{k}}_- = a\,\hat{\mathbf{p}}_+ + b\,\hat{\mathbf{p}}_- + c\,\frac{(\hat{\mathbf{p}}_+ \times \hat{\mathbf{p}}_-)}{|\hat{\mathbf{p}}_+ \times \hat{\mathbf{p}}_-|}\;, \tag{25}$$
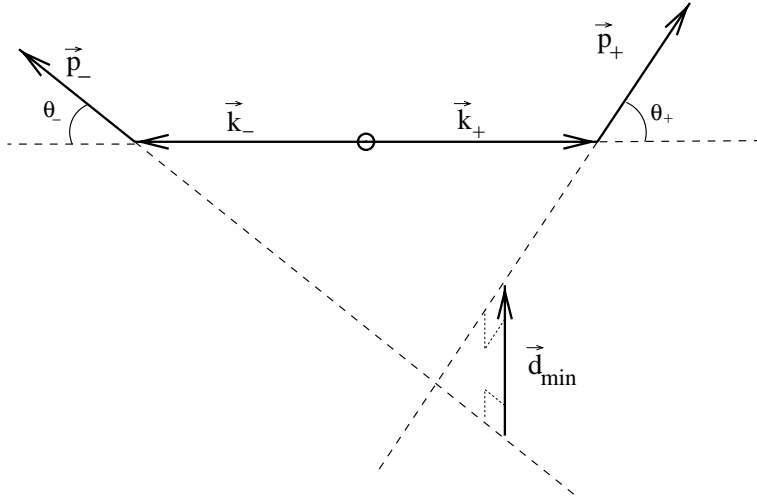
9

Figure 2: Definition of the vectors used for the τ direction reconstruction

$$a = \frac{\cos\theta_+ + (\hat{\mathbf{p}}_+ \cdot \hat{\mathbf{p}}_-)\cos\theta_-}{1 - (\hat{\mathbf{p}}_+ \cdot \hat{\mathbf{p}}_-)^2} \ , \qquad b = -\frac{\cos\theta_- + (\hat{\mathbf{p}}_+ \cdot \hat{\mathbf{p}}_-)\cos\theta_+}{1 - (\hat{\mathbf{p}}_+ \cdot \hat{\mathbf{p}}_-)^2} \ ,$$

$$c = \pm\sqrt{1 - a^2 - b^2 - 2ab(\hat{\mathbf{p}}_+ \cdot \hat{\mathbf{p}}_-)} \ ,$$

$$\cos\theta_\pm = \frac{2E_\tau E_\pm - m_\tau^2 - Q_\pm^2}{2|\vec{\mathbf{p}}_\pm|\sqrt{E_\tau^2 - m_\tau^2}} \ ,$$

where $\theta_\pm$ are the angles between the directions of the τ leptons $\hat{\mathbf{k}}_\pm$ and the hadrons $\hat{\mathbf{p}}_\pm$, $Q_\pm^2 = E_\pm^2 - \vec{\mathbf{p}}_\pm^2$, E_τ is given by the beam energy E_{beam}, and $\hat{\mathbf{p}}$ is the unit vector along $\vec{\mathbf{p}}$.

Equation 25 above reveals an ambiguity in the sign of the coefficient c. Taking into account the fact that the decay vertices of the two τ leptons are separated allows this ambiguity to be resolved. The additional information used to decide between the two solutions is provided by the sign of the scalar product of the normal to the plane defined by the two hadronic systems $(\hat{\mathbf{p}}_+ \times \hat{\mathbf{p}}_-)$ and the minimal distance $\vec{\mathbf{d}}_{\text{min}}$ of the charged tracks of the two τ decays [23, 31].

Figure 3 shows that the reconstruction of the vector $\vec{\mathbf{d}}_{\text{min}}$ is well modelled by the detector simulation. The correct solution for the sign of c is chosen in 65% of the events. In about 22% of the events the coefficient c cannot be computed due to effects like initial state radiation or detector resolution. Taking in these cases for the τ direction its projection onto the plane spanned by the two hadronic systems (by setting $c = 0$) still gives a good approximation of the true direction of flight. The resolution estimated from the Monte Carlo and averaged over all events with a reconstructed τ direction is 13.0 mrad. If only a single solution can be computed the resolution is 15.9 mrad, compared to a resolution of 12.3 mrad for the chosen direction when the coefficient c can be computed.
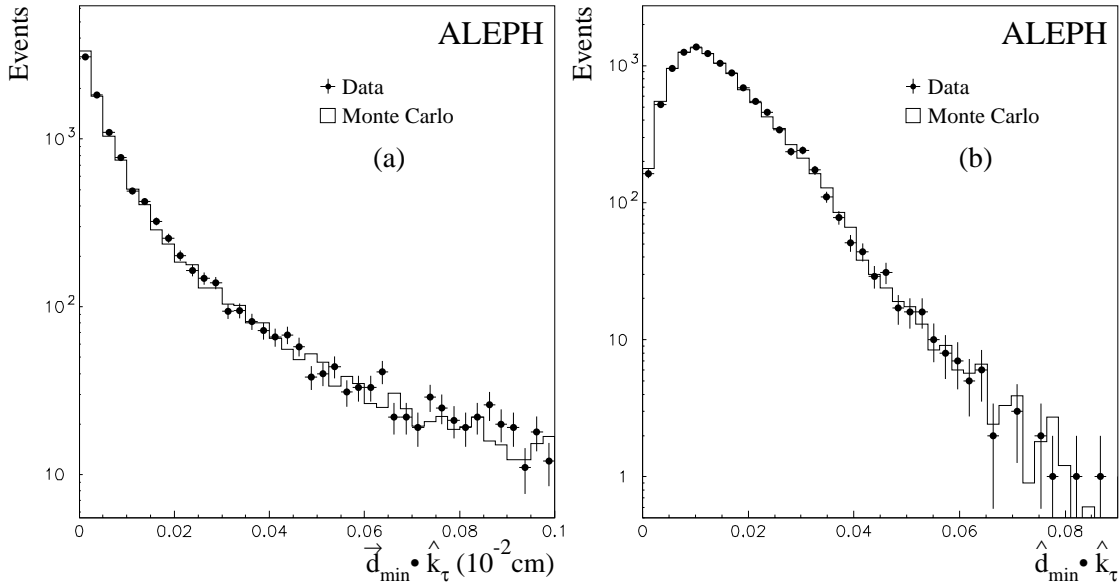
10

Figure 3: Comparison between data and Monte Carlo: a) length of the projection of $\vec{\mathrm{d}}_{\mathrm{min}}$ onto the chosen τ direction and b) cosine of the angle between $\vec{\mathrm{d}}_{\mathrm{min}}$ and $\vec{\mathrm{k}}_\tau$

6   Analysis method

As discussed in Section 2, the variables which are sensitive to the polarisation are also suitable for the measurement of the Michel parameters.

For the decay modes e, μ, and π, the reduced energy $x = E/E_{\mathrm{beam}}$ is used. For μ and π the energy is computed from the curvature of the track measured in the tracking devices, whereas for the electron the energy is measured with the wires in the ECAL including also the bremsstrahlung photons. For events with unidentified hemispheres, only the identified hemisphere information contributes to the measurement.

In the case of the final states with two or three pions, the optimal observables $\omega_\rho = G_\rho/F_\rho$ and $\omega_{a_1} = G^1_{a_1}/F_{a_1}$, defined in Section 2.2, are used. In events with both τ leptons decaying hadronically, the τ direction is reconstructed and ω is determined in each hemisphere from the full set of kinematic variables. For events with a leptonic or unidentified decay in the opposite hemisphere the τ direction is not known and hence the dependence of the functions F and G on the angle α is integrated out with a corresponding loss of sensitivity to ξ_h of the resulting ω distribution. The spectra for the various decay modes are shown in Fig. 4 with the Standard Model Monte Carlo [32] prediction.

6.1   Fitting procedure

In order to exploit the spin-spin correlation of the two τ leptons, the parameters are extracted by a binned maximum likelihood fit to two-dimensional distributions obtained from the 27 decay combinations (Table 3) which can be constructed from the six decay modes $e\bar{\nu}_e\nu_\tau$, $\mu\bar{\nu}_\mu\nu_\tau$, $\pi(K)\nu_\tau$, $\pi\pi^0\nu_\tau$, $\pi\pi^0\pi^0\nu_\tau$, $\pi\pi^+\pi^-\nu_\tau$, and unidentified decays.

11

The fit relies on simulated reference distributions which are constructed by reweighting the standard τ Monte Carlo [32]. For example, in the case of a hadron-hadron correlation, where the correlated spectrum is given by Eq. 23, they are the two-dimensional distributions $f_{h_1}f_{h_2}$, $g_{h_1}g_{h_2}$, $f_{h_1}g_{h_2}$, and $f_{h_2}g_{h_1}$. This method ensures that all effects such as radiative corrections, resolution and selection are automatically taken into account in the reference distributions. The fit of a normalized linear combination of these reference distributions to the data, by varying the coefficients, yields the values of the unknown parameters.

Assuming a Poisson distribution in the individual bins, the likelihood function is given by the following expression:

$$\mathcal{L} = \prod_{S=1}^{11} \prod_{C=1}^{27} \prod_{B=1}^{n} \frac{\exp\left(-\mathrm{E}_{S,C,B}\right)(\mathcal{P})\mathrm{E}_{S,C,B}(\mathcal{P})^{\mathrm{N}_{S,C,B}}}{\mathrm{N}_{S,C,B}!} \quad , \tag{26}$$

$$\sum_{B=1}^{n} \mathrm{E}_{S,C,B}(\mathcal{P}) = \mathrm{N}_{S,C}^{\mathrm{data}} \; .$$

The symbol $\mathcal{P} = \left(\rho_e, \xi_e, (\xi\delta)_e, \eta_\mu, \rho_\mu, \xi_\mu, (\xi\delta)_\mu, , \xi_\pi, \xi_\rho, \xi_{a_1}, P_\tau\right)$ denotes the set of parameters to be measured. The parameter η_e is set to zero and the polarisation parameter[3] P_τ is let free to avoid biases on the Michel parameters, mainly ρ_μ and ρ_e.

N is the number of events observed in the data. S runs over the 11 data samples which correspond to the five years of data taking, and running at the Z peak and at off-peak energies. The letter C designates one of the 27 decay combinations and B a data bin.

The distributions of the Z peak data are divided into 15×15 bins and, due to the lower statistics, the off-peak histograms are split into 10×10 bins only.

The expectation $\mathrm{E}_{S,C,B}(\mathcal{P})$ in each bin is obtained by the following sequence of operations.

- The reference distributions for the considered data sample and decay combination are linearly combined. The coefficients are computed from the values of the parameters which are varied during the fit.

- The distributions for τ background due to wrong decay combinations are added. The background distributions are computed for the two τ^- helicities assuming the Standard Model values of the decay parameters and their respective contributions are determined by the value of the P_τ parameter.

- The non-τ background (Bhabha events, μ pairs, hadronic events, and $\gamma\gamma$ events) is added.

- The $\mathrm{E}_{S,C,B}(\mathcal{P})$ expectation is normalized to the number of events in the data distribution.

---

[3]With the present notations, the polarisation measured in the standard analysis [23] is $\xi_h P_\tau$ for a hadronic channel and approximately $\xi_l P_\tau - (4/3)[\rho_l - 3/4]$ for a leptonic one

6.2   Results of the fit

The values of the parameters given by the maximum likelihood fit are presented in Table 4 and their correlation matrix in Table 5.

Table 4: Results of the fit with statistical errors only. The right column gives the values expected for a pure $V - A$ interaction

Parameter	Fit result	SM
ρ_e	0.747 ± 0.019	0.75
$(\xi\delta)_e$	0.788 ± 0.066	0.75
ξ_e	1.011 ± 0.094	1.00
η_μ	0.160 ± 0.150	0.00
ρ_μ	0.776 ± 0.045	0.75
$(\xi\delta)_\mu$	0.786 ± 0.066	0.75
ξ_μ	1.030 ± 0.120	1.00
ξ_π	0.994 ± 0.020	1.00
ξ_ρ	0.987 ± 0.012	1.00
ξ_{a_1}	1.000 ± 0.016	1.00

Table 5: The correlation matrix for the fit

	$(\xi\delta)_e$	ξ_e	η_μ	ρ_μ	$(\xi\delta)_\mu$	ξ_μ	ξ_π	ξ_ρ	ξ_{a_1}
ρ_e	0.00	-0.23	-0.02	0.02	0.00	-0.02	0.10	0.00	0.00
$(\xi\delta)_e$		0.05	0.01	0.00	0.00	-0.02	-0.12	0.01	0.01
ξ_e			0.01	0.01	-0.02	-0.01	-0.06	-0.02	-0.01
η_μ				0.91	0.29	0.58	0.03	-0.02	-0.01
ρ_μ					0.25	0.45	0.06	-0.02	-0.01
$(\xi\delta)_\mu$						0.14	-0.07	-0.02	-0.01
ξ_μ							-0.01	-0.04	-0.02
ξ_π								-0.28	-0.20
ξ_ρ									-0.08

The value of P_τ given by the fit is in agreement with the results of the measurement in the framework of the Standard Model [23] but with a larger error. The errors on the parameters η_μ and ρ_μ have a correlation of 91% which is due to the underlying decay distribution. As a consequence the error on ρ_μ is rather large. This is in contrast to the electron channel where the error on ρ_e is smaller because the decay distribution is insensitive to η_e. In the fit η_e has been fixed to 0; fixing also η_μ results in an error on ρ_μ comparable to that on ρ_e.

Since the constants G_l defined in Eq. 1 are related to the τ leptonic partial widths by Eq. 10, under the hypothesis of e-μ universality $G_\mu = G_e$, the η parameter is constrained by the measurement of the τ leptonic branching ratios. To impose this constraint on the
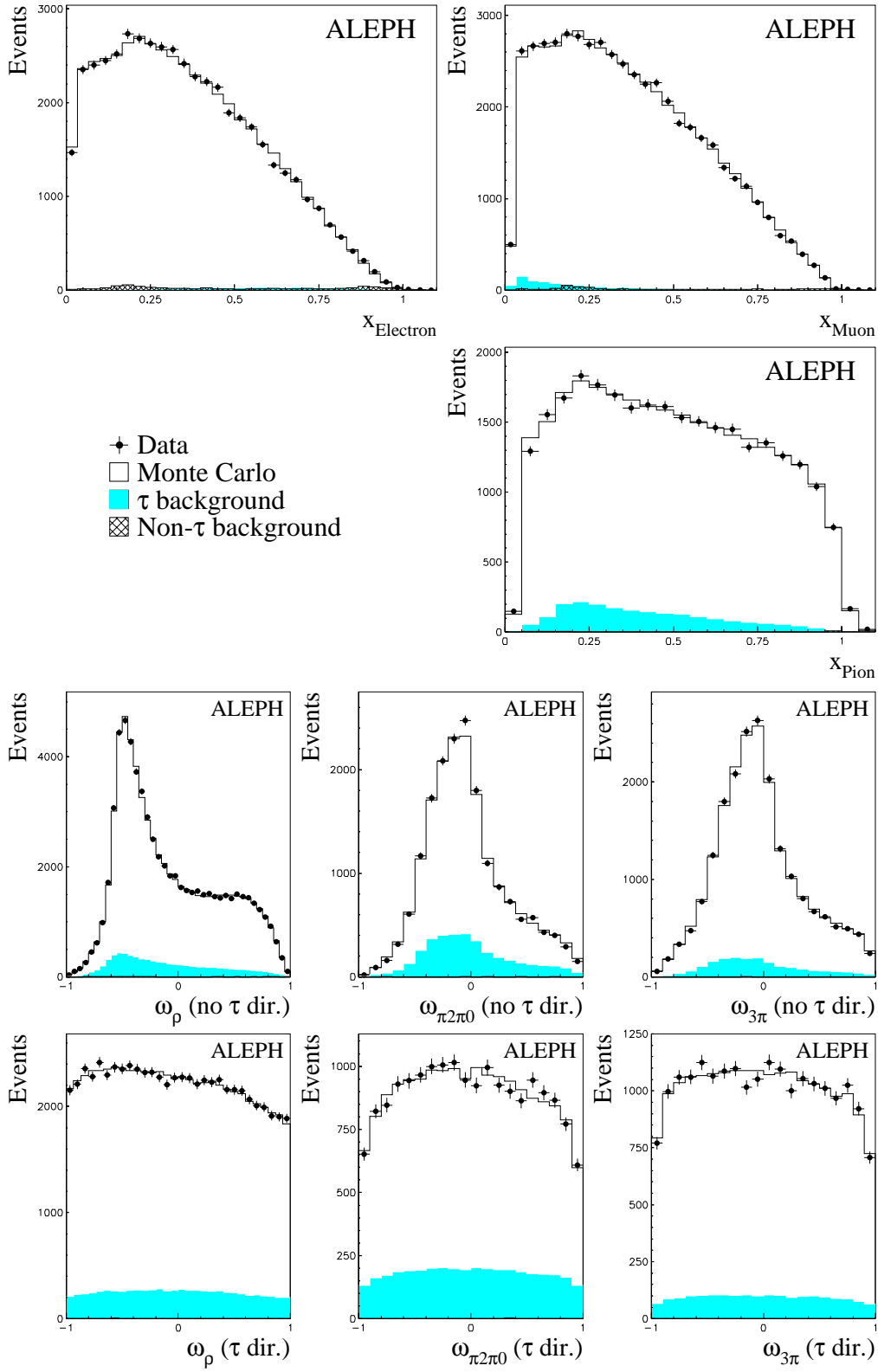
Figure 4: The kinematic variables, $x = E/E_{\text{beam}}$ for the classes e, μ, and π; the kinematic variables ω for the classes $\pi^{\pm}\pi^0, \pi^{\pm}2\pi^0$, and $3\pi^{\pm}$

14

fit, a term

$$\ln \mathcal{L}^{\mathrm{br}} = -\frac{1}{2}\frac{(\eta_l - \eta_{\mathrm{br}})^2}{(\Delta\eta_{\mathrm{br}})^2},\tag{27}$$

where η_{br} is the value of η_l deduced from the branching ratio measurements [33], is added to the log-likelihood function. The precise sensitivity of the branching ratios to η_l, needed to determine $\Delta\eta_{\mathrm{br}}$, is computed from the exact decay distribution [34], taking into account the acceptance cut on the low energy muons. The value obtained is $\eta_{\mathrm{br}} = 0.001 \pm 0.027$.

The values of the parameters given by the fit performed under the assumptions of universality and $\xi_\pi = \xi_\rho = \xi_{a_1}$ are given in Table 6 with their errors and correlations.

Table 6: Results of the fit and correlation matrix, under the assumptions of e-μ universality and $\xi_\pi = \xi_\rho = \xi_{a_1}$

Parameter	Fit result	SM
η_l	0.012 ± 0.026	0.00
ρ_l	0.742 ± 0.014	0.75
$(\xi\delta)_l$	0.776 ± 0.045	0.75
ξ_l	0.986 ± 0.068	1.00
ξ_h	0.992 ± 0.007	1.00

	ρ_l	$(\xi\delta)_l$	ξ_l	ξ_h
η_l	0.26	0.05	0.08	0.00
ρ_l		0.03	-0.19	0.10
$(\xi\delta)_l$			0.05	-0.11
ξ_l				-0.09

7   Systematic uncertainties

All systematic errors arising from the uncertainties in the Monte Carlo simulation are discussed in the following and summarized in Table 7. Illustrations of the procedures used for their determination are presented in Figs. 5 to 7. Most of the tools used in the present analysis were also employed for the measurement of the τ polarisation described in [23], where a more detailed discussion can be found.

Good calibration of the TPC and the electromagnetic calorimeter are crucial for a reliable measurement of the parameters. This analysis also profits from the thorough refinement of the TPC and ECAL calibrations using Bhabha and μ-pair events, which was done for the τ polarisation analysis [23] to reduce the related uncertainties. To estimate the uncertainties due to the TPC calibration, twice the errors on the sagitta measurement and the absolute momentum normalization are taken. The results are given in Table 7 in column "TPC".

Table 7: Systematic uncertainties in units of 10^{-2} from the following sources: momentum measurement from tracking in the magnetic field (TPC), energy measurement in the ECAL (ECAL), τ pair selection (SEL), normalization of the non-τ background (BKG), charged particle identification (PID), photon and π^0 detection efficiency (γ/π^0), Monte Carlo statistics (MC), and the τ branching fractions assumed in the Monte Carlo (τBF). The lower part of the table shows the uncertainties under the assumptions of e-μ universality and $\xi_\pi = \xi_\rho = \xi_{a_1}$

	TPC	ECAL	SEL	BKG	PID	γ/π^0	MC	τBF
ρ_e	—	0.7	0.5	0.2	0.4	—	0.7	0.4
$(\xi\delta)_e$	—	0.3	0.4	0.1	0.3	—	2.2	1.0
ξ_e	—	0.4	1.5	0.2	1.4	—	3.4	0.6
η_μ	1.5	—	0.8	0.5	2.5	—	4.9	1.7
ρ_μ	0.9	—	0.2	0.3	0.5	—	1.4	0.5
$(\xi\delta)_\mu$	0.5	—	0.6	1.0	0.9	—	2.2	1.2
ξ_μ	0.4	—	0.7	0.5	0.8	—	4.8	0.8
ξ_π	0.3	0.4	0.6	0.0	0.6	0.2	0.7	0.6
ξ_ρ	0.1	0.4	0.4	0.0	0.2	0.8	0.5	0.1
ξ_{a_1}	0.3	0.3	0.6	0.0	0.2	0.6	0.7	0.6

	TPC	ECAL	SEL	BKG	PID	γ/π^0	MC	τBF
η_l	0.1	0.1	0.1	0.1	0.4	—	0.3	0.2
ρ_l	0.1	0.1	0.2	0.1	0.3	—	0.5	0.2
$(\xi\delta)_l$	0.6	0.2	0.5	0.1	1.5	—	1.6	0.5
ξ_l	0.4	0.5	1.0	0.2	1.4	—	2.5	0.7
ξ_h	0.1	0.3	0.1	0.0	0.1	0.3	0.2	0.2

The errors arising from the ECAL are independently estimated for the wires used to measure the electron energy and the pads necessary for the identification of photons; the barrel and endcaps are also treated separately. An uncertainty due to saturated signals in the ECAL is determined by varying the measured value of the saturation constant within its error (1σ); the uncertainties on the calibration are assessed by evaluating the differences between data and Monte Carlo using Bhabha events. Finally, the uncertainty in the measurement of the photon energy in the ECAL due to the photon clustering algorithm, which affects the hadronic final states [23], is estimated. All uncertainties due to the calibration of the ECAL are combined in Table 7, column "ECAL".

The effects of the selection procedure are estimated by defining suitable test samples in data and Monte Carlo in the same way. The dependence on the relevant variables used in the measurement of the ratio data/MC of the efficiencies relative to the tests samples is studied. Whenever possible a linear fit to the ratio is performed, the error on the slope, or the slope itself if larger than the error, is then used to reweight the Monte Carlo distributions. The systematic uncertainties are estimated by redoing the fit with the new distributions. Deviations from linearity, if present, are taken into account.

For the test of the $\tau\tau$ selection a sample of lepton-lepton events is defined by loosening the cuts, especially the energy cuts. This results in a much larger fraction of background events in the critical regions around $x = 1$ and small x, which is also used to check
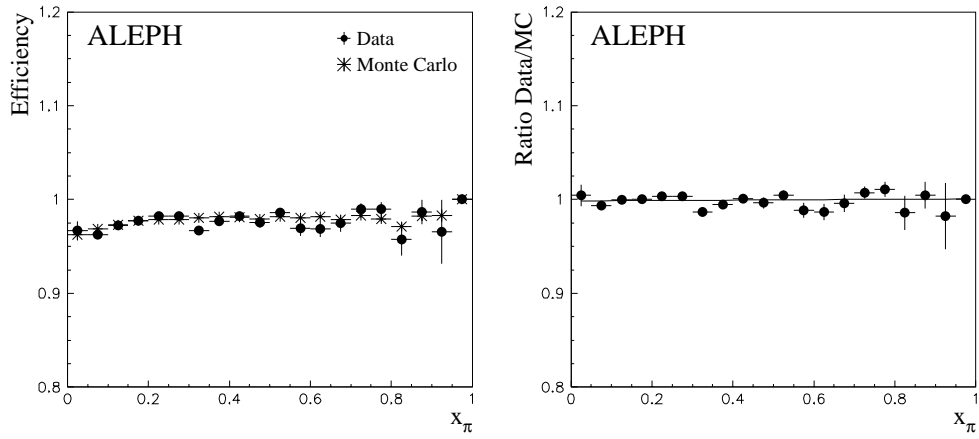
Figure 5: Comparison between data and Monte Carlo for the efficiency of the particle ID in the case of pions. The result of a linear fit of the Data/MC ratio is superimposed
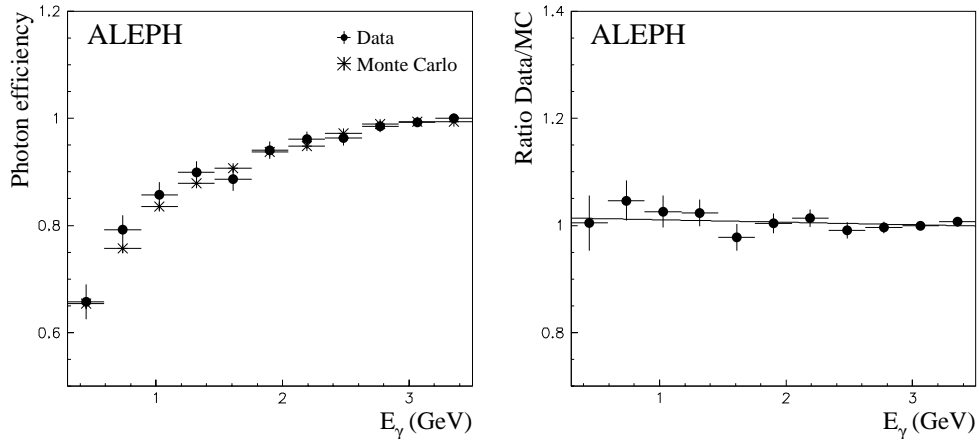

Figure 6: Comparison between data and Monte Carlo for the efficiency of the selection of good photons. The result of a linear fit of the Data/MC ratio is superimposed
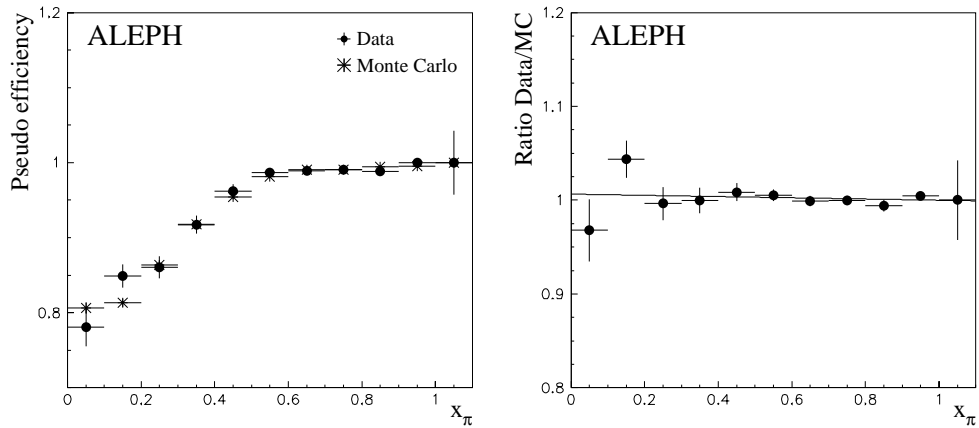

Figure 7: Comparison between data and Monte Carlo for the pseudo-efficiency of the calorimetric selection in the case of the pion class. The result of a linear fit of the Data/MC ratio is superimposed

17

the normalization of the non-τ background in the Monte Carlo. The statistical error from the comparison of data and Monte Carlo is taken as the systematic uncertainty of the background normalization. It depends on the year of data taking and ranges between 20% and 30%. The uncertainties resulting from these studies are given in Table 7, columns "SEL" and "BKG".

The identification of electrons and muons can be tested using tracks from Bhabha events, μ pairs, and $\gamma\gamma$ events with ee and $\mu\mu$ final states. Two-track events are selected using one track identified as an electron or muon to tag the track in the opposite hemisphere. In order to obtain clean test samples, cuts on the momenta of the tracks, the missing mass in the event, or the acollinearity angle are applied. In addition, muon candidates should not be accompanied by a substantial energy deposit in the ECAL. The test sample for pion identification (Fig. 5) is selected directly from τ decay. The test sample consists of tracks accompanied by clean π^0's and tracks from three-prong hemispheres, the other two tracks being identified as pions. The remaining background in the test samples is subtracted. These test samples are used to estimate the systematic errors given in Table 7, column "PID", by means of the procedure described above. The uncertainty due to particle identification also contains effects from misidentification.

The likelihood estimator used to reject fake photons might have an identification efficiency for photons which differs in data and Monte Carlo. To assess this possible effect a sample of good photons from well defined π^0's is selected by using one of the photons for tagging and the other for testing. The ratio data/MC of the efficiencies on this test sample as a function of the photon energy (Fig. 6) is used to determine the systematic uncertainty. Since there are small differences in the energy spectra of the π^0's between data and Monte Carlo, a systematic error on the π^0 reconstruction is estimated from the ratio of these spectra. Finally the uncertainties related to the additional cuts of the hemisphere identification, such as the calorimetric selection for pions, the mass cuts in two- and three-pion final states, and the cut on the number of photons for $\pi^\pm\nu_\tau$ and $3\pi^\pm\nu_\tau$ are evaluated from the ratios of "pseudo-efficiencies". These pseudo-efficiencies (Fig. 7) are the ratios of the numbers of events before and after the cut is applied. The errors resulting from these uncertainties are summarized in Table 7 in column "γ/π^0".

Differences in the reconstruction of the τ direction of flight between data and Monte Carlo should show up in the first Euler angle α (Section 2.2), which can only be computed when the τ direction is known. Therefore the distributions of this angle for data and Monte Carlo are used to assess these systematic uncertainties. The resulting errors are $\Delta\xi_\rho = \pm 0.001$ and $\Delta\xi_{a_1} = \pm 0.002$. The effects on ξ_π are negligible.

An important source of uncertainty is the finite Monte Carlo statistics used to generate the reference distributions. This error is determined by allowing the number of events in all bins to fluctuate assuming a Poisson distribution and refitting. With this procedure repeated several hundred times, the statistical error due to the Monte Carlo is given by the width of the Gaussian distributions of the individual fitted parameters. The same procedure is applied for the distributions from τ background and non-τ background. The combined errors are listed in Table 7 in column "MC".

The uncertainty coming from the branching ratios implemented in the Monte Carlo, which affects the shape of the background, is assessed by varying the branching ratios

within their errors (1σ). It appears in the column "τBF" of Table 7.

The model dependence of the hadronic current for the three-pion final states has also a systematic effect on the results. This uncertainty is evaluated, as in the τ polarisation measurement [23], by trying different models [35–37] and changing their parameters in the limits allowed by the data. Nevertheless, instead of the three $G_{a_1}^i$ functions used to construct ω_{a_1} in the τ polarisation analysis, only one function ($G_{a_1}^1$) is employed here. Variations in ξ_{a_1} between $+0.005$ and -0.020 are found, showing that at the level of precision reached now the model dependence is the dominant uncertainty on ξ_{a_1}. Since no model can be claimed to be definitely established, care must be taken in interpreting the result for ξ_{a_1} and the larger of the two values is put as theoretical systematic uncertainty in the final result.

8   Results and conclusion

A precision measurement of the Michel parameters of the τ lepton and the ν_τ helicity has been presented, exploiting the full statistics of $\tau^+\tau^-$ pairs collected with the ALEPH detector at LEP. The sensitivity to the chirality parameters ξ_ρ and ξ_{a_1} has been increased by about a factor of two by using the information from the reconstruction of the τ direction of flight. The results of this analysis, for the Michel parameters and the hadronic chirality parameters (ν_τ helicity), are

$$\rho_e = 0.747 \pm 0.019 \pm 0.014,$$
$$(\xi\delta)_e = 0.788 \pm 0.066 \pm 0.024,$$
$$\xi_e = 1.011 \pm 0.094 \pm 0.038,$$
$$\eta_\mu = 0.160 \pm 0.150 \pm 0.060,$$
$$\rho_\mu = 0.776 \pm 0.045 \pm 0.019,$$
$$(\xi\delta)_\mu = 0.786 \pm 0.066 \pm 0.028,$$
$$\xi_\mu = 1.030 \pm 0.120 \pm 0.050,$$
$$\xi_\pi = 0.994 \pm 0.020 \pm 0.014,$$
$$\xi_\rho = 0.987 \pm 0.012 \pm 0.011,$$
$$\xi_{a_1} = 1.000 \pm 0.016 \pm 0.013 \pm 0.020;$$

and, under the assumptions of e-μ universality and $\xi_\pi = \xi_\rho = \xi_{a_1}$,

$$\eta_l = 0.012 \pm 0.026 \pm 0.004,$$
$$\rho_l = 0.742 \pm 0.014 \pm 0.006,$$
$$(\xi\delta)_l = 0.776 \pm 0.045 \pm 0.024,$$
$$\xi_l = 0.986 \pm 0.068 \pm 0.031,$$
$$-\langle h_{\nu_\tau} \rangle = \xi_h = 0.992 \pm 0.007 \pm 0.006 \pm 0.005.$$

The errors are the statistical and the experimental systematic errors, the third error is due to the uncertainties in the model for the three-pion final state. The values of the

parameters defined by Equations. 7 and 8 are

$$\mathcal{S}_R^\tau = -0.023 \pm 0.031 \pm 0.016 \ , \qquad \mathcal{P}_R^\tau = -0.025 \pm 0.041 \pm 0.022$$

with a correlation coefficient $C(\mathcal{S}_R^\tau, \mathcal{P}_R^\tau) = 0.90$.

The values obtained for the Michel parameters and the ν_τ helicity are in good agreement with measurements from other experiments [17–19,38–44]. No significant deviation from the pure $V - A$ interaction assumed in the Standard Model is observed.

Acknowledgements

References

[1] W. Fetscher, H.-J. Gerber and K.-F. Johnson, Phys. Lett. B **173** (1986) 102

[2] D.-E. Groom et al. (Particle Data Group) Eur. Phys. J. C **15** (2000) 1

[3] ALEPH Collaboration, *Michel Parameters and τ Neutrino Helicity from Decay Correlations in $Z \rightarrow \tau^+\tau^-$* , Phys. Lett. B **346** (1995) 379; **363** (1995) 265 (erratum)

[4] L. Michel, Nature **163** (1949) 959; Proc. Phys. Soc. **63A** (1950) 514

[5] C. Bouchiat and L. Michel, Phys. Rev. **106** (1957) 170

[6] L. Okun and A. Rudik, Sov. Phys. JETP **5** (1957) 520

[7] T. Kinoshita and A. Sirlin, Phys. Rev. **108** (1957) 844

[8] F. Scheck, Phys. Rep. **44** (1978) 187

[9] W. Fetscher, Phys. Rev. D **42** (1990) 1544

[10] A. Rougé, Eur. Phys. J. C **18** (2001) 491

[11] J. Polak and M. Zralek, Phys. Rev. D **46** (1992) 3871

[12] W. Hollik and T. Sack, Phys. Lett. B **284** (1992) 427

[13] A. Stahl, Phys. Lett. B **324** (1994) 121

[14] M. Davier, L. Duflot, F. Le Diberder and A. Rougé, Phys. Lett. B **306** (1993) 411

[15] C.-A. Nelson, Phys. Rev. D **53** (1996) 5001; Phys. Lett. B **335** (1995) 561

[16] J.-H. Kühn and E. Mirkes, Z. Phys. C **56** (1992) 661; C **67** 364 (erratum)

[17] ARGUS Collaboration, *Determination of the tau-neutrino helicity*, Phys. Lett. B **250** (1990) 164

[18] OPAL Collaboration, *A measurement of the hadronic decay current and the ν_τ-helicity in $\tau^- \to \pi^-\pi^-\pi^+\nu_\tau$*, Z. Phys. C **75** (1997) 593

[19] CLEO Collaboration, *Hadronic Structure in the Decay $\tau^- \to \nu_\tau\pi^-\pi^0\pi^0$ and the Sign of the Tau Neutrino Helicity*, Phys. Rev. D **61** (2000) 012002

[20] H. Kühn and F. Wagner, Nucl. Phys. B **326** (1984) 16

[21] S.-Y. Pi and A.-I. Sanda, Ann. Phys. **106** (1977) 171

[22] C.-A. Nelson, Phys. Rev. D **40** (1989) 123

[23] ALEPH Collaboration, *Measurement of the Tau Polarisation at LEP*, CERN-EP/2001-027, to be published in Eur. Phys. J. C

[24] SLD Collaboration, *A High-Precision Measurement of the Left-Right Z Boson Cross-Section Asymmetry*, Phys. Rev. Lett. **84** (2000) 5945

[25] ALEPH Collaboration, *ALEPH: A Detector for Electron-Positron Annihilations at LEP*, Nucl. Instrum. and Methods A **294** (1990) 121

[26] ALEPH Collaboration, *Performance of the ALEPH detector at LEP*, Nucl. Instrum. and Methods A **360** (1995) 481

[27] ALEPH Collaboration, *Z production cross sections and lepton pair forward-backward asymmetries*, Z. Phys. C **62** (1994) 539

[28] ALEPH Collaboration, *Tau leptonic branching ratios*, Z. Phys. C **70** (1996) 561

[29] ALEPH Collaboration, *Performance of the ALEPH detector at LEP*, Nucl. Inst. and Meth. A **360** (1995) 481

[30] P. Overmann, Univ. of Dortmund, *A new method to measure the tau polarization at the Z peak*, DO-TH 93-24 (1993)

[31] J.-H. Kühn, Phys. Lett. B **313** (1993) 458

[32] S. Jadach, B.-F.-L. Ward and Z. Wąs, Comput. Phys. Commun. **79** (1994) 503

[33] ALEPH Collaboration, *Measurement of the tau leptonic branching ratios at LEP I*, ALEPH 99-014 (CONF 99-009)

[34] A.-M. Sachs and A. Sirlin, *Muon decay*, in *Muon Physics*, V.-W Hughes and C.-S. Wu eds. (Academic Press, New York 1975)

[35] N. Isgur, C. Morningstar and C. Reader, Phys. Rev. D **39** (1989) 1357

[36] J.-H. Kühn and A. Santamaria, Z. Phys. C **48** (1990) 445

[37] M. Feindt, Z. Phys. C **48** (1990) 681

[38] ARGUS Collaboration, *Determination of the Michel parameters ρ, ξ, and δ in τ-lepton decays with τ → ρν tags*, Phys. Lett. B **431** (1998) 179

[39] L3 Collaboration, *Mesurement of the Michel parameters and the average tau-neutrino helicity from tau decays at LEP*, Phys. Lett. B **438** (1998) 405

[40] SLD Collaboration, *Measurement of the τ Neutrino Helicity and Michel Parameters in Polarized e^+e^- Collisions*, Phys. Rev. Lett. **78** (1997) 4691

[41] CLEO Collaboration, *Determination of the Michel parameters and the τ neutrino helicity in τ decay*, Phys. Rev. D **56** (1997) 5320

[42] CLEO Collaboration, *A Measurement of the Michel Parameters in Leptonic Decays of the Tau*, Phys. Rev. Lett. **78** (1997) 4686

[43] OPAL Collaboration, *Measurement of the Michel Parameters in Leptonic Tau Decays*, Eur. Phys. J. C **8** (1999) 3

[44] DELPHI Collaboration, *A Study of the Lorentz Structure in Tau Decays*, Eur. Phys. J. C **16** (2000) 229